

Synthesis and characterization of mesoporous poly(*N*-vinyl-2-pyrrolidone) containing palladium nanoparticles as a novel heterogeneous organocatalyst for Heck reaction



Roozbeh Javad Kalbasi*, Meysam Negahdari

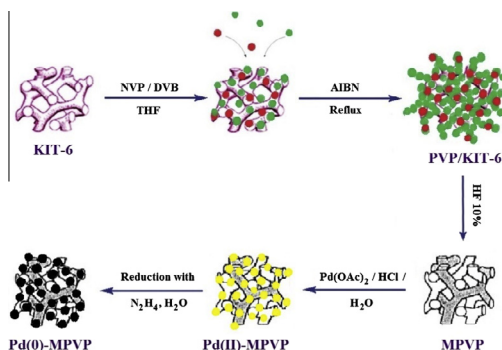
Department of Chemistry, Shahreza Branch, Islamic Azad University, 311-86145 Shahreza, Isfahan, Iran

HIGHLIGHTS

- Mesoporous poly(*N*-vinyl-2-pyrrolidone) was prepared based on mesoporous KIT-6.
- Pd-MPVP was prepared as a novel heterogeneous organocatalyst.
- The mesoporous organocatalyst was used for the Heck reaction.
- The stability of the catalyst was excellent and could be reused 9 times.

GRAPHICAL ABSTRACT

Mesoporous poly(*N*-vinyl-2-pyrrolidone) containing Pd nanoparticles was prepared and used as a novel purely organic heterogeneous catalyst. The catalyst showed high catalytic activity in Heck reaction and could be reused at least nine times.



ARTICLE INFO

Article history:

Received 19 October 2013
Received in revised form 8 January 2014
Accepted 27 January 2014
Available online 1 February 2014

Keywords:

Mesoporous polymer
Poly(*N*-vinyl-2-pyrrolidone)
Pd-nanoparticles
Heck reaction

ABSTRACT

Mesoporous poly(*N*-vinyl-2-pyrrolidone) (MPVP) was prepared through a nanocasting technique based on mesoporous silica KIT-6 as sacrificial templates, and served as an efficient scaffold for supporting Pd nanoparticles. The physical and chemical properties of Pd-MPVP were characterized using FT-IR, XRD, BET, DRS UV-Vis, SEM, TEM and TGA techniques. The application of this novel purely organic heterogeneous catalyst, which combine the advantage of organic polymers and mesoporous materials, was investigated for C–C bond formation through the Heck coupling reaction of aryl iodides, bromides and chlorides with styrene. It was observed that the activity of this catalyst decreased just 5% after nine regeneration processes were performed. This unique result opens new perspectives for application of purely organic mesoporous polymers as structurally defined hydrophobic catalyst in catalytic reactions.

© 2014 Elsevier B.V. All rights reserved.

1. Introduction

Reactions leading to the formation of C–C bonds are important to the synthesis of complex organic molecules. Among

these reactions, the Heck reaction has been widely used for construction of a carbon–carbon bond [1]. Many Pd complexes have been used as homogeneous catalysts in this reaction [2–5]. Although some of the Pd complexes have potential for recycling [2,6], the separation and recovery of most of them are not easy, and the resulting products are often contaminated by Pd metal. Thus, it is necessary to develop heterogeneous catalysts

* Corresponding author. Tel.: +98 321 3212522; fax: +98 321 3213103.

E-mail address: rkalbasi@iaush.ac.ir (R.J. Kalbasi).

which can easily be recovered from the reaction system and re-used [7–10].

In heterogeneous catalysts, various support matrices such as organic polymers [11–13] and inorganic silicas, especially porous inorganic materials with high surface areas, have been employed [14–16]. Compared with organic polymers, inorganic supports with nanopores can provide high surface area, large pore volume, and 3-dimensional pore architecture, which are favorable for mass transfer in catalysis. However, the disadvantages of inorganic supports including relatively low stability in alkaline media and complex functionalization of them are challenges for preparation of heterogeneous catalysts with high activity and excellent recyclability. For example, Si–O–Si bonds in ordered mesoporous silicas are not stable in alkaline media, and immobilization of palladium species on silica surface generally requires unique organic linkers [17,18]. On the other hand, the organic mesoporous materials with some significant advantages such as flexibility, toughness, hydrophobicity and versatility for further functionalization are quite different from their inorganic counterparts as a result of the intrinsic characteristics of organic molecules [19].

Mesoporous polymeric materials have gained much attention for the adsorption, separation, and catalysis of large molecules [20–22], and also as dielectric materials [23], due to their high specific surface area [24,25], uniform pore diameter [26–29], and chemical stability for recyclability [30,31]. Nevertheless, among the different researches on these materials, there are relatively a few reports on the application of mesoporous polymeric materials as a heterogeneous catalyst [32–37]. Mesoporous polymers can be prepared by various routes, including phase separation [38,39], controlled foaming [40,41], imprinting with large molecules or nanoparticles [42,43], ion track etching [44], selective decomposition within a block copolymer assembly [45–48], assembly of resin precursors by surfactants [26,28,29], and polymerization inside a removable porous template or with embedded template particles [49,50]. Among these methods, the porous template method is also referred to as 'hard-templating', 'nanocasting', or 'template synthesis'. Most synthetic strategies for fabricating mesoporous polymers have been dependent on the hard template approach [51–53]. The template mesoporous polymeric replicas are obtained after the selective removal of the silica framework in the polymer/silica composites. In this way, a porous polymeric material is obtained.

In continuing our previous activities to develop new mesoporous polymers as heterogeneous catalysts [54], herein, we will introduce a novel mesoporous polymer as a heterogeneous catalyst prepared using a cubic-type mesoporous silica template with 3D porous networks. The catalytic activity of this catalyst (Pd-mesoporous poly(*N*-vinyl-2-pyrrolidone)) was tested for Heck reaction in aqueous medium under aerobic condition. In addition, the catalytic activity of this mesoporous polymeric catalyst was compared with polymer–inorganic hybrid materials which were prepared in our previous works [55,56], to investigate the advantages of mesoporous polymeric catalysts.

2. Materials and methods

2.1. Chemicals supply

N-vinyl-2-pyrrolidone (VP, 97%) as monomers, *p*-Divinylbenzene (DVB, 85%) as crosslinker and 2,2'-azobis(isobutyronitrile) (AIBN) as initiator were purchased from Sigma–Aldrich. All other chemicals were obtained from Sigma–Aldrich, Merck and were used without further purification.

2.2. Catalyst preparation

2.2.1. Preparation of KIT-6

Synthesis of mesoporous silica KIT-6 was obtained following the method reported by Kleitz et al. [57]. Briefly, 6 g (1.03 mmol) of triblock copolymer Pluronic P123 (EO₂₀PO₇₀EO₂₀) (as a soft template and structure directing agent to preparation of KIT-6) and 6 g (81 mmol) of *n*-butanol were dissolved in 270 g (15 mol) of distilled water and 11.4 g (0.115 mol) of concentrated hydrochloric acid (37 wt% HCl). The mixture was left stirring at 35 °C for 1 h. Then 12.9 g (0.061 mol) of tetraethyl orthosilicate (TEOS) was added to the homogeneous clear solution. This mixture was left stirring at 45 °C for 24 h for the formation of mesostructured product, followed by aging at 95 °C for 24 h under a stirring condition. The solid product was then filtered, washed with deionized water and dried at 100 °C. Finally, the samples were calcined at 550 °C for 6 h to remove the template.

2.2.2. Preparation of mesoporous poly(*N*-vinyl-2-pyrrolidone)

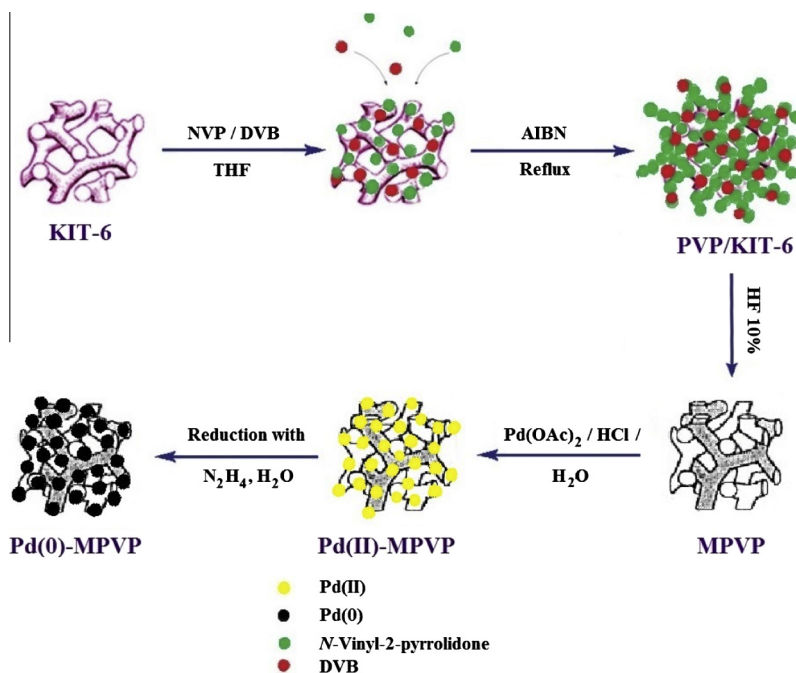
Poly(*N*-vinyl-2-pyrrolidone) (PVP) was deposited inside the porosity of KIT-6. This was carried out by *in situ* polymerization. As a typical run, at first, *N*-vinyl-2-pyrrolidone (NVP) (1 mL, 9.2 mmol), KIT-6 (0.5 g) and Divinylbenzene (0.061 mL, 0.441 mmol) in 7 mL tetrahydrofuran (THF) were placed in a round bottom flask. The solution was stirred with magnetic stirrer and refluxed for 6 h at 65 °C to achieve a uniform distribution of organic monomers inside the pores of KIT-6 prior to polymerization. Then, 2,2'-azobis(isobutyronitrile) (AIBN) (5 mol% with respect to VP) was added to start the polymerization and the mixture was heated to 65–70 °C for 17 h while being stirred under N₂ gas. The resulting white fine powder nanocomposite (PVP/KIT-6) was collected by filtration, washed several times with THF to remove remaining monomers, and finally dried at 60 °C under reduced pressure. The resulting PVP/KIT-6 nanocomposite was immersed in a 10 wt% HF solution (water/ethanol = 1/1) at room temperature for 18 h to remove the silica framework. Then, it was filtered and washed sequentially with water/ethanol solution and the precipitate was dried in room temperature to yield mesoporous poly(*N*-vinyl-2-pyrrolidone). The synthesized mesoporous poly(*N*-vinyl-2-pyrrolidone) was briefly denoted as MPVP.

2.2.3. Preparation of Pd nanoparticle–mesoporous poly(*N*-vinyl-2-pyrrolidone)

Mesoporous poly(*N*-vinyl-2-pyrrolidone) (MPVP) (0.25 g) and 10 mL of an aqueous acidic solution (C_{HCl} = 0.09 M) of Pd(OAc)₂ (0.0066 g, 0.029 mmol) were placed in a round bottom flask. The mixture was heated to 80 °C for 5 h while being stirred under N₂ gas. Then, 0.15 mL (2.47 mmol) aqueous solutions of hydrazine hydrate (N₂H₄·H₂O) (80 vol.%) was added to the mixture drop by drop in 15–20 min. After that, the solution was stirred at 60 °C for 1 h. Afterwards, it was filtered and washed sequentially with chloroform and methanol to remove excess N₂H₄·H₂O, and was dried at room temperature to yield palladium nanoparticle–mesoporous poly(*N*-vinyl-2-pyrrolidone) (Pd-MPVP) (Scheme 1). The Pd content of the catalyst was estimated by decomposing the known amount of the catalyst by nitric acid, hydro-chloric acid, and Pd content was estimated by inductively coupled plasma atomic emission spectrometry (ICP-AES). The Pd content of the catalyst estimated by ICP-AES was 0.0864 mmol g⁻¹.

2.3. Instruments and characterization

The samples were analyzed using FT-IR spectroscopy (using a Perkin Elmer 65 in KBr matrix in the range of 4000–400 cm⁻¹). The BET specific surface areas and BJH pore size distribution of the samples were determined by adsorption–desorption of



Scheme 1. Schematic showing the procedure for the preparation of Pd-MPVP.

nitrogen at liquid nitrogen temperature, using a Series BEL SORP 18. The X-ray powder diffraction (XRD) of the catalyst was carried out on a Bruker D8Advance X-ray diffractometer using nickel filtered Cu K α radiation at 40 kV and 20 mA. The thermal gravimetric analysis (TGA) data were obtained by a Setaram Labsys TG (STA) in a temperature range of 30–700 °C and heating rate of 10 °C/min in N₂ atmosphere. Scanning electron microscope (SEM) studies were performed on Philips, XL30, SE detector. Transmission electron microscope (TEM) observations were performed on a JEOL JEM.2011 electron microscope at an accelerating voltage of 200 kV using EX24093JGT detector in order to obtain information on the size of Pd nanoparticles and the DRS UV-Vis spectra were recorded with JASCO spectrometer, V-670 from 190 to 2700 nm.

The products were characterized by ¹H NMR and ¹³C NMR spectra (Bruker DRX-500 Avance spectrometer at 400 and 100 MHz, respectively). Melting points were measured on an Electrothermal 9100 apparatus and they were uncorrected. All the products were known compounds and they were characterized by FT-IR, ¹H NMR and ¹³C NMR. All melting points are compared satisfactorily with those reported in the literature.

2.4. General procedure for Heck reaction

In the typical procedure for Heck coupling reaction, a mixture of iodobenzene (1 mmol), styrene (2 mmol), K₂CO₃ (5 mmol), and catalyst (0.14 g, Pd-MPVP) in MeOH/H₂O (volume ratio: 3:1) (5 mL) was placed in a round bottom flask. The suspension was stirred at 45 °C for 4 h. The progress of reaction was monitored by TLC using n-hexane as eluent. After completion of the reaction (monitored by TLC), for the reaction work-up, the catalyst was removed from the reaction mixture by filtration, and then the reaction product was extracted with CH₂Cl₂ (3 mL × 5 mL). The solvent was removed under reduced pressure. The crude product was purified by flash column chromatography to afford the desired coupling product (97% isolated yield). The product was identified with ¹H NMR, ¹³C NMR and FT-IR spectroscopy techniques.

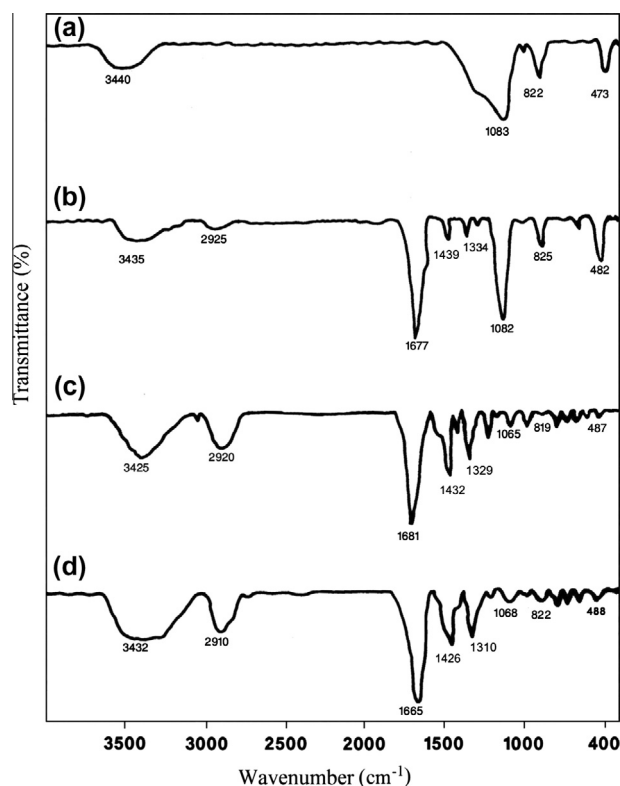


Fig. 1. FT-IR spectra of (a) mesoporous silica KIT-6, (b) PVP/KIT-6, (c) MPVP and (d) Pd-MPVP.

3. Results and discussion

3.1. Catalyst characterization

Fig. 1 presents the FT-IR spectra of KIT-6 (a), PVP/KIT-6 (b), MPVP (c), and Pd-MPVP (d). A broad band at around 3400–3450 cm⁻¹ is observed in all samples. It is mainly caused by the

O–H stretching vibration of the adsorbed water molecules. The characteristic bands at around 1080, 820 and 480 cm^{-1} may be assigned to Si–O–Si asymmetrical stretching vibration, symmetrical stretching vibration and bending vibration, respectively, as seen in Fig. 1a and b. The existence of PVP in the PVP/KIT-6 composite is evidenced by the appearance of typical PVP vibration on the FT-IR spectrum (Fig. 1b). In the FT-IR spectrum of PVP/KIT-6, the new band at 1677 cm^{-1} corresponds to the carbonyl bond of PVP [58]. Moreover, the presence of peaks at around 2900–3000 cm^{-1} and 1439 cm^{-1} correspond to the aliphatic C–H stretching and bending in PVP/KIT-6, respectively. The appearance of the above bands shows that PVP has been attached to the surface of KIT-6 and PVP/KIT-6 has been obtained. Similar to PVP/KIT-6 (Fig. 2b), MPVP sample shows the characteristic bands for PVP, while the bands at around 1080, 820 and 480 cm^{-1} which are related to the asymmetric and symmetric stretching as well as the rocking of Si–O–Si are omitted (Fig. 2c). These results have shown that the silica framework has been successfully removed and MPVP has been prepared as a replica of KIT-6.

As shown in Pd-MPVP spectrum (Fig. 1d), the band at 1681 cm^{-1} which corresponds to carbonyl bond of PVP, is shifted to lower wave numbers (1665 cm^{-1}) (red shift). This may be due to the interaction between the Pd nanoparticles and C=O group. This means that the double bond CO stretches become weak by coordinating to Pd nanoparticles [58,59]. Thus, it is confirmed that PVP molecules exist on the surface of the Pd nanoparticles and coordinate to the Pd nanoparticles.

The low angle XRD patterns of KIT-6, PVP/KIT-6, MPVP and Pd-MPVP are shown in Fig. 2. The XRD pattern of KIT-6 (Fig. 2a) shows one intense peak at 2θ about 0.95° and two weak peaks at 2θ about 1.65° and 1.9° which can be indexed as (211), (220), and (320) reflections associated with three-dimensional cubic symmetry

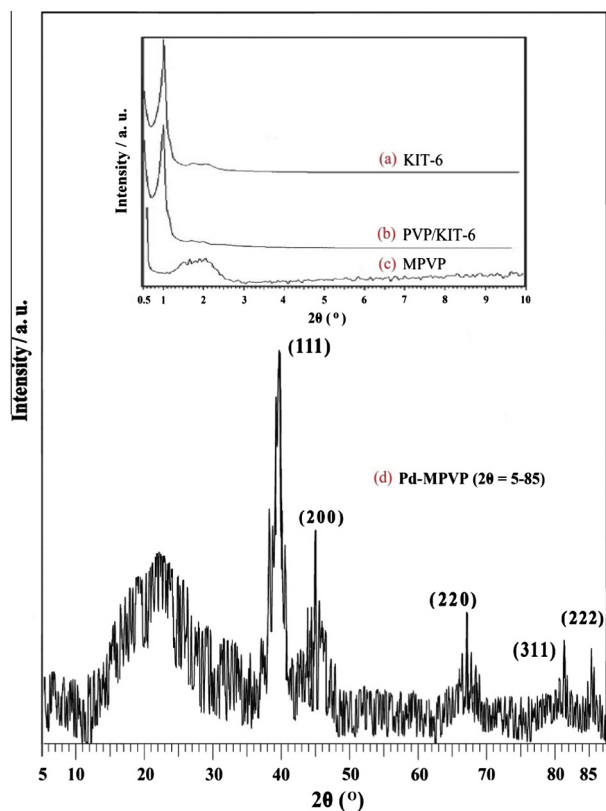


Fig. 2. Powder XRD patterns of (a) mesoporous silica KIT-6, (b) PVP/KIT-6, (c) MPVP, and (d) Pd-MPVP.

Table 1

Physicochemical properties of mesoporous silica KIT-6, PVP/KIT-6, MPVP and Pd-MPVP samples obtained from N_2 adsorption.

Sample	BET surface area ($\text{m}^2 \text{g}^{-1}$)	V_p ($\text{cm}^3 \text{g}^{-1}$) ^a	D_p (nm)
KIT-6	988	1.35	8.1
PVP/KIT-6	794	1.17	7.1
MPVP	226	0.52	4.2
Pd-MPVP	168	0.11	3.3

^a Total pore volume.

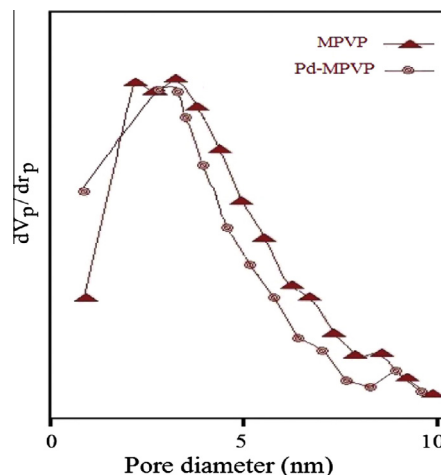


Fig. 3. Pore size distribution of MPVP and Pd-MPVP.

($1a3d$) [60]. The PVP/KIT-6 ($2\theta = 0.6$ – 10) sample show the same pattern indicating that the structure of the KIT-6 is retained even after the support of the surface of the KIT-6 with PVP (Fig. 2b). The pattern of MPVP shows a typical mesoporous structure with a peak at 2θ around 1.5–2.5° corresponding to a mesoporous framework. However, the peak position is shifted to a higher angle (in comparison to KIT-6) which can be attributed to a decrease in the dimension of d-spacing (the inter-planar spacing) of MPVP, according to the Bragg's law. However, it can be expected because MPVP is a negative replica of KIT-6 [51]. Moreover, the intensity and sharpness of the characteristic reflection peak of MPVP is reduced, indicating the loss of long-range order to some extent because of organic nature of MPVP.

The wide angle XRD pattern of the Pd-MPVP (Fig. 2d) shows the reflections at $2\theta = 39.92^\circ$, 46.54° , 67.90° , 81.84° and 85.50° . These peaks correspond to (111), (200), (220), (311) and (222) lattice planes of Pd nanoparticles [61]. Planes were assigned by comparing them with the standard Pd and these planes correspond to the fcc crystal lattice structure of Pd (JCPDS, Card No. 05-0681). The pattern displays a broad diffraction with 2θ ranging from 15° to 30°, which suggests the amorphous structure of the polymeric base. The crystallite size of Pd particles was evaluated using Scherrer equation which was found to be approx. 5 nm in size. The size of the Pd nanoparticles, determined by using TEM analysis, is more reliable than that determined by using Scherrer formula in XRD analysis. It should be mentioned that the wide-angle XRD pattern of Pd-MPVP is similar to MPVP (data not shown).

The BET specific surface areas, the pore volumes and the pore sizes of KIT-6, PVP/KIT-6, MPVP and Pd-MPVP samples were calculated using BET and BJH methods (Table 1). The surface area, pore volume and pore size of KIT-6 are $988 \text{ m}^2 \text{g}^{-1}$, $1.35 \text{ cm}^3 \text{g}^{-1}$, and 8.1 nm, respectively. After hybridization with PVP through *in situ* polymerization, PVP/KIT-6 exhibits a smaller pore size and pore volume than those of KIT-6, which may be concluded that polymerization of PVP occurs in the channels of the KIT-6.

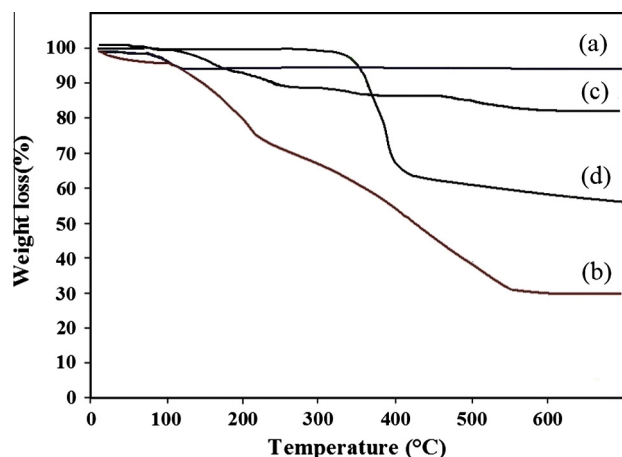


Fig. 4. TGA curves of (a) mesoporous silica KIT-6, (b) PVP (nonporous), (c) PVP/KIT-6 and (d) MPVP.

The corresponding BJH pore size distribution curves for the MPVP and Pd-MPVP materials are shown in Fig. 3. As it can be seen, MPVP which is obtained after the selective removal of the silica template from PVP/KIT-6, exhibits a relatively narrow pore size distribution centered at 4.2 nm. However, the pore size distribution of MPVP is smaller than that of KIT-6 which is expected and it is in good agreement with the XRD result (shift of peak position to a higher angle). Although the specific surface area of MPVP ($226 \text{ m}^2 \text{ g}^{-1}$) is smaller than that of PVP/KIT-6 (Table 1), MPVP still has a large channel-like pores and a high surface area which indicates that MPVP is a true replica of the mesoporous silica KIT-6, and makes it suitable to act as a mesoporous organic support. In this regard, Pd-MPVP exhibits a relatively narrow pore size distribution like MPVP, which means that Pd nanoparticles are well distributed on the channels and surfaces of MPVP (Fig. 3 and Table 1). Moreover, Pd-MPVP has a reasonable surface area, pore size and

pore volume which makes it suitable to act as a catalyst for Heck reaction.

The TGA curves of the KIT-6 (a), PVP (non-porous) (b), PVP/KIT-6 (c) and MPVP (d) under N_2 atmosphere are presented in Fig. 4. The TGA curve of KIT-6 shows a small mass loss (around 5%, w/w) at temperature $<150^\circ\text{C}$, which is apparently associated with adsorbed water on the surfaces of KIT-6. No other changes in the weight are observed for KIT-6 at $150\text{--}700^\circ\text{C}$ (Fig. 4a). However, TG curve of PVP (non-porous) shows 2 steps; the first step (around 5%, w/w) appearing at temperature $50\text{--}120^\circ\text{C}$ corresponds to the loss of water. The second weight loss (around 65%, w/w) begins at 150°C because of thermo degradation of PVP polymer chains, and the degradation ends at 550°C (Fig. 4b).

Thermo analysis of PVP/KIT-6 shows two steps of mass loss (Fig. 4c). The first step (around 2%, w/w) that occurs at temperatures less than 150°C is related to desorption of water. The second step (around 15%, w/w) which appears at 170°C is attributed to degradation of the polymer chains, and the degradation ends at 570°C (Fig. 4c). MPVP sample exhibits just one weight loss step (around 40%, w/w), which begins at 350°C because of thermo degradation of PVP polymer chains, and the degradation ends at 600°C (Fig. 4d). Obviously, the MPVP shows a higher thermal stability than that of PVP (nonporous), which may be related to the ordered mesoporous structure of MPVP. Actually, the ordered structure of MPVP causes to increase the degree of crystallinity of the polymer (producing semi crystalline form) and thermal stability of MPVP is increased. Therefore, it is very important for the catalyst application that the thermal stability be enhanced greatly.

The morphological characteristics of KIT-6, MPVP and Pd-MPVP which are illustrated by the SEM microphotographs are shown in Fig. 5. A comparison of MPVP (Fig. 5b) with KIT-6 template (Fig. 5a) reveals that the morphology of the silica template is relatively retained in the mesoporous polymer. This suggests that with the appropriate template it may be possible to prepare polymeric structure with a pre-selected shape.

By comparing the SEM images of MPVP and Pd-MPVP, we can see that there are some agglomerate particles (lighter spots) on

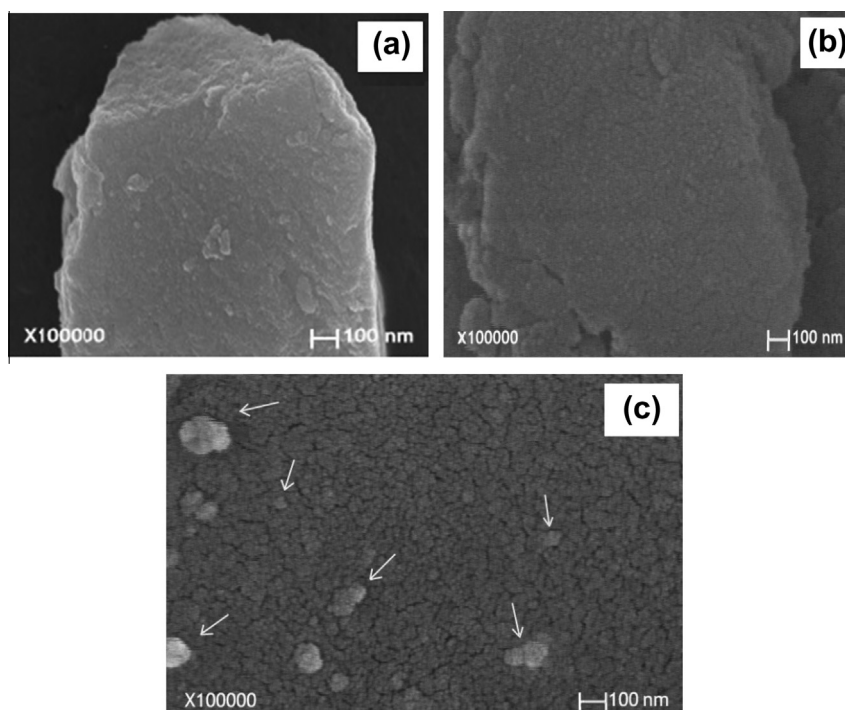


Fig. 5. SEM photographs of (a) KIT-6, (b) MPVP and (c) Pd-MPVP.

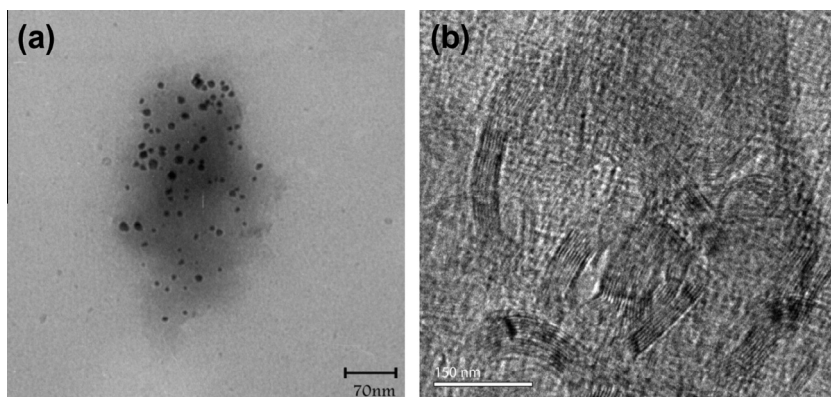


Fig. 6. TEM images of Pd-MPVP.

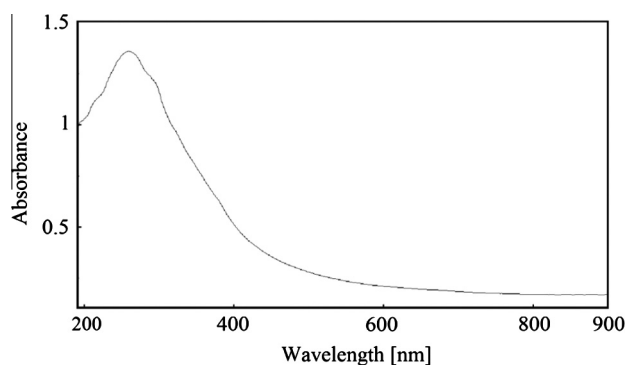


Fig. 7. UV-Vis spectrum of Pd-MPVP.

the surface of Pd-MPVP which are related to the Pd nanoparticles distributed on the outer surface of the support (Fig. 5c).

The TEM micrographs of Pd-MPVP are depicted in Fig. 6. TEM experiment demonstrates that palladium nanoparticles were uniformly dispersed on the surface of MPVP (Fig. 6). This is due to the existence of a large number of organic groups, as anchoring sites, on the surface of MPVP. The places with darker contrast can be assigned to the presence of Pd particles with different dispersion. The small dark spots in the image can be ascribed to Pd nanoparticles with average diameter around ~4 nm (Fig. 6), probably located into the support channels. The dark spherical particles most likely correspond to Pd nanoparticles which are located on the external surface with average diameter of ~10–18 nm or more than that (40–120 nm according to SEM results) (Fig. 6). These are in accordance with SEM results.

Fig. 7 displays the result of UV-Vis spectrum of Pd-MPVP. Normally, the UV-Vis spectrum of Pd(OAc)₂, reveals a peak at 400 nm

Table 2
Effects of various solvents on Heck reaction^{a,b}.

Solvent	Yield ^c (%)
Methanol/water (3:1 v/v)	97
Methanol	92
Water	80
Dioxane	60
Acetonitrile	67

^a Reaction conditions: Pd-MPVP (0.14 g), iodobenzene (1 mmol), styrene (2 mmol), K₂CO₃ (5 mmol), solvent (5 mL), 45 °C, 4 h.

^b *E/Z* stereoselectivity was higher than 99:1 (determined by ¹H NMR spectroscopy).

^c Isolated yield of the *E* isomer.

Table 3
Effect of different bases on Heck reaction^{a,b}.

Base	Yield ^c (%)
None	Trace
K ₂ CO ₃	97
Na ₃ PO ₄	70
Et ₃ N	50

^a Reaction conditions: Pd-MPVP (0.14 g), iodobenzene (1 mmol), styrene (2 mmol), base (5 mmol), MeOH/H₂O (5 mL), 45 °C, 4 h.

^b *E/Z* stereoselectivity was higher than 99:1 (determined by ¹H NMR spectroscopy).

^c Isolated yield of the *E* isomer.

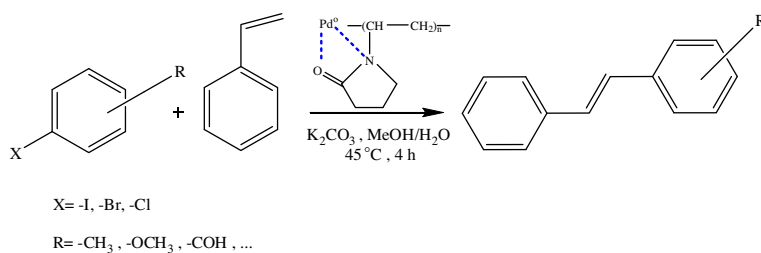
which is referred to the existence of Pd(II) [62]. As mentioned in Section 2, Pd-MPVP is prepared by adding hydrazine hydrate to the Pd(II)-mp-PVP. However, as can be seen in Fig. 7, there is no peak at 400 nm in the UV-Vis spectrum of Pd-MPVP, which indicates complete reduction of Pd(II) to Pd nanoparticles.

3.2. Catalytic activity

This novel organocatalyst was synthesized and characterized with different methods. The main goal of this catalytic synthesis was to compare this purely organic nanocatalyst (Pd-MPVP) with a polymer-inorganic nanocomposite (Pd-PVP/KIT-6, which was prepared in our previous work [56]) or respective non-porous polymer (Pd-PVP) and to expand the use of these types of purely organic nanocatalyst for organic reactions. High thermal stability, high surface areas, narrow pore size distributions, regular frameworks and hydrophobic surface nature of Pd-MPVP are some of advantages of this nanocatalyst which make it as a good candidate to catalyze organic reactions. In this regard, a Heck reaction of various aryl halides with styrene under aerobic condition was chosen to test the catalytic activity of Pd-MPVP as a purely organic nanocatalyst.

To optimize the reaction conditions, a model reaction was carried out by taking iodobenzene and styrene in different solvents and bases at 45 °C. Solvent plays a crucial role in the rate and product distribution of Heck reactions. In this context, we used a kind of solvents; and the reaction was catalyzed with 0.14 g of Pd-MPVP (containing about 0.92 wt% palladium) (Table 2). The experimental results showed that the time it took for the reaction to be completed was rarely shorter in the case of using MeOH/H₂O (3:1, v/v) as a solvent and the yield was higher. Hence, MeOH/H₂O (3:1, v/v) was chosen as optimized solvent.

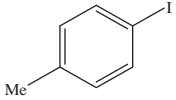
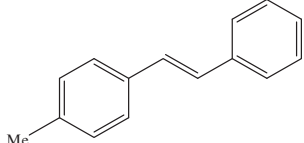
Careful selection of the base in terms of its solubility and basicity in the reaction mixture was crucial. The role of the base in the

Table 4Heck reaction of aromatic aryl halides and styrene catalyzed by Pd-MPVP^{a,b}

Entry	Substrate	Product	Yield (%) ^c	Time (h)	TOF (h ⁻¹) ^d	Mp (°C)	
						Found	Rep. Ref.
1			97	4	20.04	120–122	122–123 [64]
2			97	8 ^e	10.02	120–122	122–123 [64]
3			93	6	12.81	120–122	122–123 [64]
4			87	7	10.27	131–135	135.4–137.1 [64]
5			78	4 ^e	16.11	111–114	115–116 [64]
6			82	5 ^e	13.55	138–141	140–144 [64]
7			76	6	10.46	115–118	117–119 [65]
8			90	6	12.39	72–73	71–72 [66]

(continued on next page)

Table 4 (continued)

Entry	Substrate	Product	Yield (%) ^c	Time (h)	TOF (h ⁻¹) ^d	Mp (°C)	
						Found	Rep. Ref.
9			84	7	9.91	117–119	116–118 [67]

^a Reaction conditions: Pd-MPVP (0.14 g), aryl halide (1 mmol), styrene (2 mmol), K₂CO₃ (5 mmol), MeOH/H₂O (3:1 v/v) (5 mL), 45 °C.

^b *E/Z* stereoselectivity was higher than 99:1 (determined by ¹H NMR spectroscopy).

^c Isolated yield of the *E* isomer.

^d Turn-over frequency.

^e Reflux condition.

Table 5

Catalyst reusability for the Heck reaction^{a,b}.

Cycle	Yield (%) ^c	Pd content of catalyst (mmol in 0.14 g) ^d
Fresh	97	0.0121
1	97	0.0121
2	97	0.0121
3	97	0.0119
4	97	0.0119
5	95	0.0118
6	95	0.0118
7	95	0.0118
8	92	0.0117
9	92	0.0116

^a Reaction conditions: Pd-MPVP, iodobenzene (1 mmol), styrene (2 mmol), K₂CO₃ (5 mmol), MeOH/H₂O (3:1 v/v) (5 mL), 45 °C, 4 h.

^b *E/Z* stereoselectivity was higher than 99:1 (determined by ¹H NMR spectroscopy).

^c Isolated yield of the *E* isomer.

^d Measured by ICP-AES.

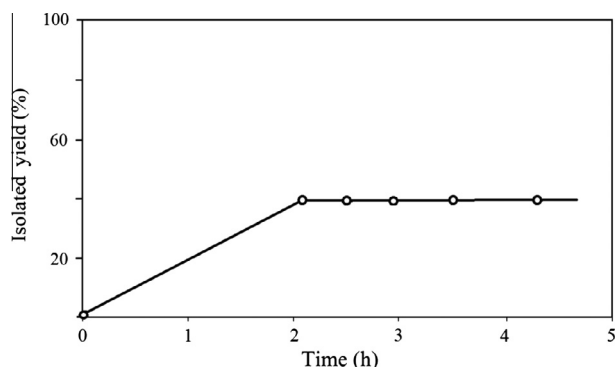


Fig. 8. Heterogeneity test for Heck coupling reaction. Reaction conditions: Pd-MPVP (0.14 g), iodobenzene (1 mmol), styrene (2 mmol), K₂CO₃ (5 mmol), MeOH/H₂O (3:1 v/v), 45 °C.

mechanistic cycle is to reactivate the Pd species in solution, making it available to be recycled [63]. The results revealed that the inorganic bases used were more effective than Et₃N (Table 3), most probably due to their complete solubility in solvent. Hence, cheaper K₂CO₃ was chosen as the base for the coupling reactions. From the data obtained, it can be concluded that the nature of the base play a significant role in the conversion using Pd-MPVP as the catalyst. These observations agree with a previous report in the literature [2].

In order to discriminate the effect of the support (MPVP), the reaction occurred over palladium nanoparticles or MPVP in the same reaction conditions, and no activity was seen in this condition. In addition, in the absence of the catalyst, there were not

Table 6

Comparison of catalytic activity in Heck reaction over different catalysts.

Catalyst	Time (h)	Yield (%) ^a	TOF (h ⁻¹) ^b	Ref.
Pd-MPVP	4 ^c	97	20.04	This work
Pd-PVP/KIT	8 ^d	97	0.88	56
Pd-PVP (non-porous)	4 ^e	93 ^f	–	70

^a Isolated yield of the *E* isomer.

^b Turn-over frequency.

^c Reaction conditions: Pd-MPVP (0.14 g, 0.92 wt% palladium), iodobenzene (1 mmol), styrene (2 mmol), K₂CO₃ (5 mmol), MeOH/H₂O (3:1, v/v) (5 mL), 45 °C.

^d Reaction conditions: Pd-PVP/KIT-6 (0.14 g, 10.5 wt% palladium), iodobenzene (1 mmol), styrene (2 mmol), K₂CO₃ (5 mmol), MeOH/H₂O (3:1, v/v) (5 mL), 60 °C.

^e Reaction conditions: Pd-PVP (1 wt% palladium), iodobenzene (1 mmol); styrene (1.2 mmol), K₂CO₃ (2 mmol), ethanol (2.0 mL), 80 °C.

^f GC-MS yield to the *E* isomer.

any products. These results show the important role of the support and catalyst in this reaction.

In further studies, Heck reactions of a wide range of other aryl halides with styrene with 0.14 g of Pd-MPVP as catalyst were conducted under similar conditions [64–67]. The results are shown in Table 4. It is observed that the reaction goes well not only with aryl iodides and bromides but also with aryl chlorides. It is well known that activation of C–Cl bond is much more difficult than C–Br and C–I bonds, and in general requires harsher reaction conditions in heterogeneous catalysis system [8,68,69]. Therefore, activation of aryl chlorides remains a major challenge which has to be met by a highly active catalyst system. However, chlorobenzene afforded excellent coupling product over Pd-MPVP as catalyst (entry 2), but needed more time and temperature than that of aryl iodide and aryl bromide. Additionally, when aryl halides are changed with electron donating and withdrawing groups, the Pd-MPVP catalyst is still active (76–87% yield, entries 4–7 and 9), suggesting a good suitability for this catalyst in Heck reaction. Furthermore, when both bromo and chloro groups are present in the reactant, chemo selective reaction is possible. For example, *meta*-bromochlorobenzene reacts with styrene to form *meta*-chlorostilbene in 90% yield (entry 8). So, Pd-MPVP can be act as a chemo selective catalyst.

Another important issue concerning the application of a heterogeneous catalyst is its reusability and stability under reaction conditions. To gain insight into this issue, catalyst recycling experiments were carried out using a Heck reaction of iodobenzene and styrene over Pd-MPVP. The results are shown in Table 5. After each cycle, the catalyst was filtered off, washed with water (10 mL) diethylether and acetone (3 times with 5 mL). Then, it was dried in an oven at 60 °C and reused in Heck reaction. It should be mentioned that after each run, some of the catalyst was lost in the filtration process. Therefore, to solve this problem, after each run the amount of remaining catalyst was determined and the molar ratio

of the reactants was changed according to the remaining amount of catalyst.

The results show that Pd-MPVP can be reused without any modification 9 times, and no significant loss of activity/selectivity performance is observed. Moreover, there is low Pd leaching (about 4.1%) during the reaction and the catalyst exhibits high stability even after 9 recycles (Table 5).

In order to prove the heterogeneous nature of the catalyst and the absence of Pd leaching, a heterogeneity test was performed, in which the catalyst was separated from the reaction mixture at approximately 50% conversion of the starting material through centrifugation. Then, the reaction progress in the filtrate was monitored (Fig. 8). No further coupling reaction occurred even at extended times, indicating that the nature of reaction process is heterogeneous and there is not any progress for the reaction in homogeneous phase.

The catalytic activity of MPVP in Heck reaction was compared with Pd-PVP/KIT-6 nanocomposite (prepared in our previous work) [56]. The results are presented in Table 6. As it can be seen, Pd-MPVP shows higher activity in Heck reaction at shorter time and milder condition (45 °C). It can be related to the hydrophobic nature of Pd-MPVP in compared with Pd-PVP/KIT-6. It should be mentioned that Pd-MPVP is hydrophobe and Pd-PVP/KIT-6 because of existence of KIT-6, is hydrophile. Therefore, the organic reactants have more tend to adsorbed on the surface of Pd-MPVP and consequently the yield and TOF (Turn-Over-Frequency) will be higher in the case of using Pd-MPVP as catalyst.

In addition, the catalytic activities of Pd-MPVP (prepared in this work) and Pd-PVP (non-porous) were compared (Table 6) [70]. As it can be seen, Pd-MPVP shows relatively higher activity in Heck reaction at milder condition (45 °C in compare with 80 °C). Moreover, the important issue is that Pd-MPVP is completely heterogeneous in the solution (it may be because of its porous and ordered structure); while Pd-PVP (non-porous) is completely homogeneous (the separation and recovery of homogeneous are not easy). Therefore, as it is presented in Table 5, Pd-MPVP can be reused 9 times (without any modification) without significant loss of activity.

4. Conclusion

In this study, the synthesis of a novel mesoporous polymer containing Pd nanoparticles was reported. The catalytic activity of this novel catalyst was tested for Heck reaction of aryl chlorides, bromides and iodides at 45 °C under aerobic conditions. This novel purely organic heterogeneous catalyst showed following advantages: (a) high catalytic activity under mild reaction conditions; (b) easy separation of the catalyst after reaction; (c) reusability of the catalyst for several times without any loss in the yield of the reaction. In addition, comparison of catalytic activity of Pd-MPVP was done with Pd-PVP/KIT-6 (as a polymer–inorganic nanocomposite) and Pd-PVP (as a non-porous polymeric catalyst). The results showed superior activity and reusability of Pd-MPVP, which it was attributable to high surface area, hydrophobic surface nature and heterogeneity of Pd-MPVP. Finally, we believe that the new heterogeneous organocatalyst reported here would greatly contribute to an environment-friendly process.

Acknowledgements

The support by the Islamic Azad University, Shahreza Branch (IAUSH) Research Council and Center of Excellence in Chemistry is gratefully acknowledged.

References

- [1] A. Molnar, *Chem. Rev.* 111 (2011) 2251.
- [2] D. Sawant, Y. Wagh, K. Bhatte, A. Panda, B. Bhanage, *Tetrahedron Lett.* 52 (2011) 2390.
- [3] Y. Cui, L. Zhang, *J. Mol. Catal. A: Chem.* 237 (2005) 120.
- [4] M. Shi, H. Qian, *Tetrahedron* 61 (2005) 4949.
- [5] M.L. Kantam, P.V. Reddy, P. Srinivas, S. Bhargava, *Tetrahedron Lett.* 52 (2011) 4490.
- [6] F. Berthiol, H. Doucet, M. Santelli, *Tetrahedron Lett.* 45 (2004) 5633.
- [7] S.S. Prockl, W. Kleist, K. Kohler, *Tetrahedron* 61 (2005) 9855.
- [8] L. Yin, J. Liebscher, *Chem. Rev.* 107 (2007) 133.
- [9] R.J. Kalbasi, N. Mosaddegh, A. Abbaspourrad, *Tetrahedron Lett.* 53 (2012) 3763.
- [10] R.J. Kalbasi, N. Mosaddegh, A. Abbaspourrad, *Appl. Catal. A: Gen.* 423 (2012) 78.
- [11] C. Evangelisti, N. Panziera, P. Pertici, G. Vitulli, P. Salvadori, C. Battocchio, G. Polzonetti, *J. Catal.* 262 (2009) 287.
- [12] G.M. Neelgund, A. Oki, *Appl. Catal. A: Gen.* 399 (2011) 154.
- [13] J. Lu, P.H. Toy, *Chem. Rev.* 109 (2009) 815.
- [14] P. Wang, X. Zheng, *Powder Technol.* 210 (2011) 115.
- [15] Y. Feng, L. Li, Y. Li, W. Zhao, J. Gu, J. Shi, *J. Mol. Catal. A: Chem.* 322 (2010) 50.
- [16] V. Meynen, P. Cool, E.F. Vansant, *Microporous Mesoporous Mater.* 125 (2009) 170.
- [17] Jan. Demel, *J. Mol. Catal. A: Chem.* 302 (2009) 28.
- [18] B. Karimi, D. Enders, *Org. Lett.* 8 (2006) 1237–1240.
- [19] A.B. Fuertes, M. Sevilla, S. Alvarez, T. Valdes-Solis, *Microporous Mesoporous Mater.* 112 (2008) 319.
- [20] A.P. Katsoulidis, M.G. Kanatzidis, *Chem. Mater.* 24 (2012) 471.
- [21] Y. Wang, U. Gosele, M. Steinhart, *Chem. Mater.* 20 (2008) 379.
- [22] H. Deng, D.L. Gin, R.C. Smith, *J. Am. Chem. Soc.* 120 (1998) 3522.
- [23] J.L. Hedrick, R.D. Miller, C.J. Hawker, K.R. Carter, W. Volksen, D.Y. Yoon, M. Trollsas, *Adv. Mater.* 10 (1998) 1049.
- [24] F. Zhang, Y. Meng, D. Gu, Y. Yan, C.Z. Yu, B. Tu, D.Y. Zhao, *J. Am. Chem. Soc.* 127 (2005) 13508.
- [25] Y.K. Takahara, S. Ikeda, K. Tachi, T. Sakata, T. Hasegawa, H. Mori, M. Matsumura, B. Ohtani, *Chem. Commun.* (2005) 4205.
- [26] J. Jang, J. Bae, *Chem. Commun.* (2005) 1200.
- [27] J. Jang, J. Bae, *J. Non-Cryst. Solids* 352 (2006) 3979.
- [28] Y. Meng, D. Gu, F.Q. Zhang, Y.F. Shi, H. Yang, Z. Li, C.Z. Yu, B. Tu, D.Y. Zhao, *Angew. Chem. Int. Ed.* 44 (2005) 7053.
- [29] Y. Meng, D. Gu, F. Zhang, Y. Shi, L. Cheng, D. Feng, Z. Wu, Z. Chen, Y. Wan, A. Stein, D. Zhao, *Chem. Mater.* 18 (2006) 4447.
- [30] R. Drake, D.C. Sherrington, S.J. Thomson, *React. Funct. Polym.* 60 (2004) 65.
- [31] Z.M. Michalska, B. Ostaszewski, J. Zientarska, J.M. Rynkowski, *J. Mol. Catal. A: Chem.* 185 (2002) 279.
- [32] A. Modak, J. Mondal, M. Sasidharan, A. Bhaumik, *Green Chem.* 13 (2011) 1317.
- [33] N. Salam, J. Mondal, J. Mondal, A.S. Roy, A. Bhaumik, S.M. Islam, *RSC Adv.* 2 (2012) 6464.
- [34] I. Muylaert, M. Borgers, E. Bruneel, J. Schaubroeck, F. Verpoort, P. Van Der Voort, *Chem. Commun.* (2008) 4475.
- [35] P. Xia, F. Liu, C. Wang, S. Zuo, C. Qi, *Catal. Commun.* 26 (2012) 140.
- [36] S. Zhang, Q. Liu, M. Shen, B. Hu, Q. Chen, H. Li, J.P. Amoureux, *Dalton Trans.* 41 (2012) 4692.
- [37] R. Xing, Y. Liu, H. Wu, X. Li, Mingyuan He, P. Wu, *Chem. Commun.* (2008) 6297.
- [38] J. Rzaev, M.A. Hillmyer, *J. Am. Chem. Soc.* 127 (2005) 13373.
- [39] S.A. Jenekhe, X.L. Chen, *Science* 283 (1999) 372.
- [40] B. Krause, H.J.P. Sijbesma, P. Munuklu, N.F.A. Van Der Vegt, M. Wessling, *Macromolecules* 34 (2001) 8792.
- [41] B. Krause, G.H. Koops, N.F.A. Van Der Vegt, M. Wessling, M. Wubbenhorst, *J. Van Turnhout, Adv. Mater.* 14 (2002) 1041.
- [42] H.P. Hentze, M. Antonietti, *Curr. Opin. Solid State Mater. Sci.* 5 (2001) 343.
- [43] G. Wulff, *Chem. Rev.* 102 (2002) 1.
- [44] C.R. Martin, *Chem. Mater.* 8 (1996) 1739.
- [45] R.C. Smith, W.M. Fischer, D.L. Gin, *J. Am. Chem. Soc.* 119 (1997) 4092.
- [46] B.A. Pindzola, B.P. Hoag, D.L. Gin, *J. Am. Chem. Soc.* 123 (2001) 4617.
- [47] A.S. Zalusky, R. Olayo-Valles, C.J. Taylor, M.A. Hillmyer, *J. Am. Chem. Soc.* 123 (2001) 1519.
- [48] A.S. Zalusky, R. Olayo-Valles, J.H. Wolf, M.A. Hillmyer, *J. Am. Chem. Soc.* 124 (2002) 12761.
- [49] P. Jiang, K.S. Hwang, D.M. Mittleman, J.F. Bertone, V.L. Colvin, *J. Am. Chem. Soc.* 121 (1999) 11630.
- [50] D. Wu, F. Xu, B. Sun, R. Fu, H. He, K. Matyjaszewski, *Chem. Rev.* 112 (2012) 3959.
- [51] D.H. Choi, R. Ryoo, *J. Mater. Chem.* 20 (2010) 5544.
- [52] A. Wilke, J. Weber, *Macromol. Rapid Commun.* 33 (2012) 785.
- [53] A.B. Fuertes, M. Sevilla, S. Alvarez, T.V. Solis, P. Tartaj, *Adv. Funct. Mater.* 17 (2007) 2321.
- [54] R.J. Kalbasi, M. Kolahdozan, S. Mozafari, *Mater. Chem. Phys.* 138 (2012) 427.
- [55] R.J. Kalbasi, N. Mosaddegh, *Mater. Res. Bull.* 47 (2012) 160.
- [56] R.J. Kalbasi, N. Mosaddegh, *C. R. Chim.* 15 (2012) 988.
- [57] F. Kleitz, S.H. Choi, R. Ryoo, *Chem. Commun.* 17 (2003) 2136.
- [58] T. Iwamoto, K. Matsumoto, T. Matsushita, M. Inokuchi, N. Toshima, *J. Colloid Interface Sci.* 336 (2009) 879.
- [59] O. Metin, S. Ozkar, *J. Mol. Catal. A: Chem.* 295 (2008) 39.
- [60] Y. Teng, X. Wu, Q. Zhou, C. Chen, H. Zhao, M. Lan, *Sens. Actuators B* 142 (2009) 267.
- [61] P. Wang, Z. Wang, J. Li, Y. Bai, *Microporous Mesoporous Mater.* 116 (2008) 400.
- [62] P.A. Namini, A.A. Babaluo, B. Bayati, *Int. J. Nanosci. Nanotechnol.* 3 (2007) 37.

- [63] G.T. Crisp, *Chem. Soc. Rev.* 27 (1998) 427.
- [64] N. Iranpoor, H. Firouzabadi, R. Azadi, *Eur. J. Org. Chem.* (2007) 2197.
- [65] L. Wang, H. Li, P. Li, *Tetrahedron* 65 (2009) 364.
- [66] Y. Leng, F. Yang, K. Wei, Y. Wu, *Tetrahedron* 66 (2010) 1244.
- [67] N. Iranpoor, H. Firouzabadi, A. Tarassoli, M. Fereidoonzhad, *Tetrahedron* 66 (2010) 2415.
- [68] A.F. Littke, G.C. Fu, *Angew. Chem.* 114 (2002) 4350.
- [69] R. Martin, S.L. Buchwald, *Acc. Chem. Res.* 41 (2008) 1461.
- [70] D.L. Martins, H.M. Alvarez, L.C.S. Aguiar, O.A.C. Antunes, *Appl. Catal. A: Gen.* 408 (2011) 47.